Strain effect on transport properties of hexagonal boron–nitride nanoribbons*

Chen Feng(陈 风), ChenYuan-Ping(陈元平)†, Zhang Mi(张 迷), and Zhong Jian-Xin(钟建新)‡

Laboratory for Quantum Engineering and Micro-Nano Energy Technology and Department of Physics, Xiangtan University, Xiangtan 411105, *China*

(Received 17 December 2009; revised manuscript received 21 January 2010)

The transport properties of hexagonal boron–nitride nanoribbons under the uniaxial strain are investigated by the Green's function method. We find that the transport properties of armchair boron–nitride nanoribbon strongly depend on the strain. In particular, the features of the conductance steps such as position and width are significantly changed by strain. As a strong tensile strain is exerted on the nanoribbon, the highest conductance step disappears and subsequently a dip emerges instead. The energy band structure and the local current density of armchair boron–nitride nanoribbon under strain are calculated and analysed in detail to explain these characteristics. In addition, the effect of strain on the conductance of zigzag boron–nitride nanoribbon is weaker than that of armchair boron nitride nanoribbon.

Keywords: transport properties, hexagonal boron–nitride nanoribbons, Green's function

PACC: 6146, 7360

1. Introduction

Recently, the single layer of hexagonal boron–nitride (h-BN), an isostructure of graphene, has been obtained experimentally[1−3] and shown to possess excellent electronic and optical properties.[4−6] Based on the single-layer structure, boron–nitride nanoribbons (BNNRs) with different widths and edges can be produced by the same experimental process as graphene nanoribbons (GNRs).[7−12] BNNR as an analogy to GNR exhibits excellent electronic properties ruled by π-electrons in a hexagonal lattice, such as the extremely high carrier mobility.[13] Furthermore, BNNR has its own unique properties due to the large ionicity of boron (B) and nitride (N). For example, the BNNRs with different edges, i.e., armchair BNNR (A-BNNR) and zigzag BNNR (Z-BNNR), are both wide-band-gap semiconductors and promising materials in optics and opto-electronics.[14] While high thermal and chemical stabilities of BNNRs indicate that the nanoribbons may have more practical significance as electronic devices.[15] Thus, BNNRs recently have attracted intensive interest.

Many theoretical studies indicate that the strain effect is an effective way to modulate the electronic structures of nano-sheet and nanoribbon.[16−18] Our group has investigated the electronic structures of graphene under different planar strains. The results clarify that the asymmetrical strain successfully results in the opening of band-gap at the Fermi level in graphene.[16] Subsequently, Sun *et al.* studied electronic structures of GNRs under uniaxial strain. They illustrated that the band-gaps of armchair GNR underwent a zigzag oscillation under strain, while the electronic structures of zigzag GNR were not sensitive to the strain.[17] Obviously, the effect of strain on the GNRs and that on graphene are different, and GNRs with different edges have different responses to strain. Recently, our group explored electronic structures of h-BN nano-sheet under different planar strains. The calculations show that the band-gap width of the h-BN nano-sheet can be distinctly reduced by strain and the gap feature exhibits strong anisotropic behaviours.[18] In view of the various responses of nano-sheet and nanoribbon to strain, it is reasonable to expect that the electronic structures of BNNRs under strain are different from those of h-BN nano-sheet under strain. Moreover, the different electronic structures are anticipated to induce unique transport properties of BNNRs under strain.

*Project supported by the Cultivation Fund of the Key Scientific and Technical Innovation Project, Ministry of Education of China (Grant No. 708068), the Specialized Research Fund for the Doctoral Program of Higher Education, Ministry of Education of China (Grant No. 200805301001), and the Open Fund based on Innovation Platform of Hunan Colleges and Universities, China (Grant No. 09K034).

†Corresponding author. E-mail: chenyp@xtu.edu.cn

†E-mail: jxzhong@xtu.edu.cn

© 2010 Chinese Physical Society and IOP Publishing Ltd

In this paper, the transport properties of BNNRs under the uniaxial strain are investigated by the Green's function method.[19−22] First, we calculate the conductances of A-BNNR under various strains. The results show that the position and the width of the conductance steps change with strain. In particular, the highest conductance step disappears and a dip emerges instead when the tensile strain is strong enough. By analysing the energy band structure and the local current density, it is found that these phenomena originate from the redistribution of transmission channels. Meanwhile, the band-gap of A-BNNR displays a width-dependent zigzag oscillation similar to that of GNR. Then, the conductances of Z-BNNR under strain are studied. Although the strain also results in the changes of conductance steps, the effect of strain on the conductance of Z-BNNR is weaker than that of A-BNNR.

2. Model and method

The considered structures include two kinds of geometries: A-BNNR and Z-BNNR, as sketched in Fig. 1, in which W denotes the width of BNNR. Along the axial direction of BNNR, we divide the structure into three parts: a central region consisting of a finite BNNR and two semi-infinite (left and right) leads on the two sides of the central region. To calculate the electronic properties of BNNRs, the tight-binding model is needed in order to describe Hamiltonians $H_{\rm A}$ of A-BNNR and $H_{\rm Z}$ of Z-BNNR, respectively, as

$$H_{\rm A} = \varepsilon_{\rm B}\sum_i a_i^\dagger a_i + \varepsilon_{\rm N}\sum_j b_j^\dagger b_j + V_\alpha \sum_{\langle i,j\rangle}(a_i^\dagger b_j + {\rm H.c}) + V_\beta \sum_{\langle i,m\rangle}(a_i^\dagger b_m + {\rm H.c}), \quad (1)$$

$$H_{\rm Z} = \varepsilon_{\rm B}\sum_i a_i^\dagger a_i + \varepsilon_{\rm N}\sum_j b_j^\dagger b_j + V'_\alpha \sum_{\langle i,j\rangle}(a_i^\dagger b_j + {\rm H.c}) + V'_\beta \sum_{\langle i,m\rangle}(a_i^\dagger b_m + {\rm H.c}), \quad (2)$$

where $\varepsilon_{\rm B} = 2.315$ eV and $\varepsilon_{\rm N} = -2.315$ eV separately denote the on-site energies of B and N atoms.[23] $a_i^\dagger$ ($b_j^\dagger$) is the creation operator at site i (j) of B (N) atom. V_α (V'_α) and V_β (V'_β) describe the hopping energies parallel and perpendicular to the axial direction of A-BNNR (Z-BNNR), respectively. The sums in $\langle i,j\rangle$ and $\langle i,m\rangle$ are restricted to the nearest-neighbour atoms parallel and perpendicular to the axial direction of BNNR respectively. One can use the lattice Green's function method to calculate the transport properties of BNNRs. According to the Green's function scheme, the Green's function of BNNR can be expressed as[20]

$$G_{\rm s} = (E - H_0 - \Sigma_{\rm L} - \Sigma_{\rm R})^{-1}, \quad (3)$$

where H_0 is the Hamiltonian of the central region; $\Sigma_{\rm L/R} = H_1^\dagger g_{\rm L/R} H_1$ denotes the self-energy term of left or right lead; H_1 is the interaction matrix between lead and central region; $g_{\rm L/R}$ is the Green's function of left or right lead, which can be obtained based on the recursive Green's function method (RGF).[19,24] Once the total Green's function is calculated, one can obtain the conductance G of BNNRs

$$G = \frac{2e^2}{h}{\rm Tr}\left(\Gamma_{\rm L} G_{\rm s}^\dagger \Gamma_{\rm R} G_{\rm s}\right), \quad (4)$$

where $\Gamma_{\rm L,R} = {\rm i}\left(\Sigma_{\rm L,R} - \Sigma_{\rm L,R}^*\right)$ is the coupling function of left or right lead. In addition, energy band structure and local current density of BNNRs under strain can be obtained by the Green's function.[25,26]

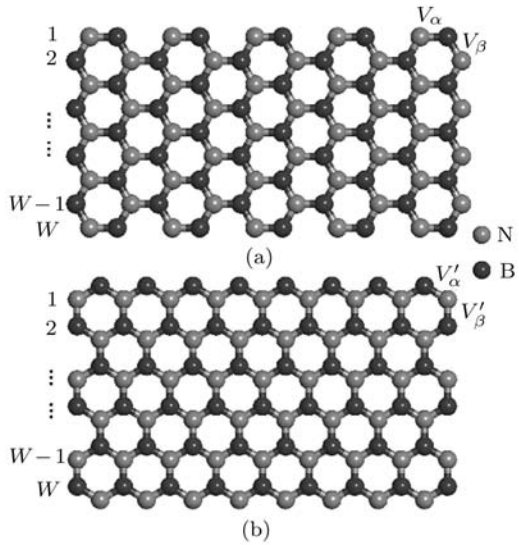


Fig. 1. (a) An A-BNNR; (b) A Z-BNNR. W denotes the width of nanoribbon. The grey and the black balls separately denote N and B atoms.

In our calculations, the hopping energies are set as $V_\alpha = V_\beta = -2.4$ eV and $V'_\alpha = V'_\beta = -2.4$ eV in the absent of strain. When a strain is exerted on BNNRs, B–N bond lengths will change with strain. The changes inevitably affect the hopping energies in BNNRs ($V_\alpha, V_\beta, V'_\alpha, V'_\beta$). The first-principles calculations clarify that the B–N bond lengths change almost linearly with strain.[27] For simplicity, we assume that the change in hopping energy is proportional to the change in B–N bond length linearly and $\Delta V_\beta = 0.13\Delta V_\alpha = 0.13t, \Delta V'_\beta = 0.25\Delta V'_\alpha = 0.25t$. In

the following discussion, we use t to denote the strain. $t < 0$ eV and $t > 0$ eV correspond to compressive and tensile strains, respectively.

3. Results and discussion

Figure 2 illustrates the conductances of A-BNNR under different values of strain t each as a function of electron energy. In Fig. 2(a), we show the conductance without strain, i.e. $t = 0$ eV. It is found that the conductance exhibits a perfect stepwise profile and a wide-band-gap exists around the Fermi energy. The maximum value of conductance is $4G_0$ ($G_0 = 2e^2/h$) that reflects the number of transmission channels in the nanoribbon. Figures 2(b) and 2(c), and 2(d)–2(f) show the conductances under compressive and tensile strains, respectively. One can find that the conductances of A-BNNR under various strains are different. Obviously, the position and the width of conductance steps change with strain strength. As a compressive strain is exerted on the nanoribbon, the width of the highest conductance step and the total spectrum range increase with strain strength [see Figs. 2(b) and 2(c)]. When a tensile strain is exerted, however, the highest step becomes narrow and the total spectrum range decreases as shown in Figs. 2(d) and 2(e). If tensile strain is strong enough, the $4G_0$ conductance step even disappears and a dip emerges in the conductance step instead [see Fig. 2(f)]. Meanwhile, one can find that the band-gap slightly changes with strain. These results indicate that the transport properties of A-BNNR are very sensitive to the strain exerted on the structure.

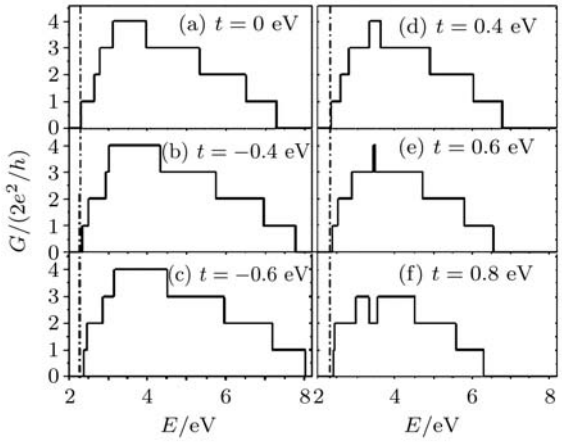


Fig. 2. Curves for conductance versus electron energy for A-BNNR with $W = 8$ under some different values of strain t. The dash lines each are a benchmark for comparison.

The transport properties of the nanoribbon are closely related to the energy band structure.[26,28] In order to explain the dependence of conductance step on strain, in Fig. 3, we show the energy band structures and the corresponding conductances of A-BNNR under different strains. One can find that the value of conductance step is related to the number of sub-bands. Without strain, i.e. when $t = 0$ eV, there are four sub-bands in the crossover part of the two sub-bands marked by 1, 2 as shown in Fig. 3(a). Thus, a $4G_0$ conductance step appears in the corresponding region of conductance profile [see Fig. 3(b)]. As a tensile strain is exerted, the symmetry of the nanoribbon is broken so that all of the sub-bands shift (upwards or downwards) with the strain. Especially, the sub-bands 1 and 2 move downwards and upwards with tensile strain respectively. Furthermore, the moving distance increases with the strength of strain. When the strain reaches 0.635 eV, the two sub-bands 1 and 2 are overlapped with each other as shown by the solid line in Fig. 3(c). This directly causes one transmission channel to die out. Consequently, the highest conductance step with $4G_0$ disappears [Fig. 3(d)]. As the strain continues to increase ($t = 0.8$ eV), the further moving of sub-bands leads sub-bands 1 and 2 to be separated as shown in Fig. 3(e) and thus a dip with $2G_0$ emerges in conductance that is denoted by the solid line in Fig. 3(f).

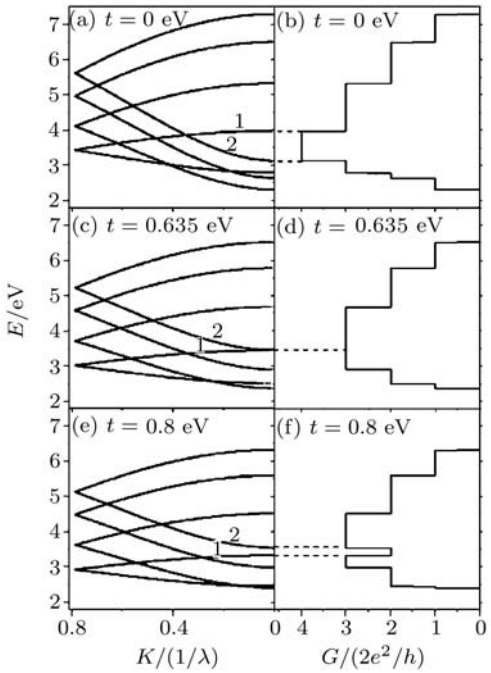


Fig. 3. Energy band structures for A-BNNR with $W = 8$ under different values of strain t. (a) $t = 0$ eV, (c) $t = 0.635$ eV and (e) $t = 0.8$ eV. (b), (d) and (f) show conductances of A-BNNR corresponding to (a), (c) and (e), respectively.

To further characterize the nature of the transport properties of A-BNNR, we explore the local current density of the structure under different values of strain t. Figure 4 displays the local current-density distributions. Clearly, the spatial characters of the plots exhibit the variations of transmission channels in the nanoribbon. In Fig. 4(a), four well-separated transmission channels emerge in nanoribbon without strain, and each of them has the same weight, which corresponds to the $4G_0$ conductance step as shown by the solid line in Fig. 3(b). When a tensile strain is exerted on the nanoribbon, the number of transmission channels decreases due to the symmetry breaking. As $t = 0.635$ eV [see Fig. 4(b)], the two middle well-separated propagating channels obviously couple together, and thus one channel vanishes. So, the value of conductance becomes $3G_0$ as shown in Fig. 3(d). While the strain increases to 0.8 eV [Fig. 4(c)], only two new well-separated channels occur in nanoribbon. Consequently, the value of conductance turns to be $2G_0$, and a dip emerges in conductance as shown by the solid line in Fig. 3(f). These results clearly indicate that the features of the electronic structures under strain are directly reflected from the transport properties of A-BNNR.

As claimed above, the band-gap of A-BNNR is slightly changed with strain t. We further investigate the dependences of band-gap on strain and ribbon width. Figure 5 illustrates the variations of band-gaps of A-BNNRs with strain t for different widths. From Fig. 5(a), one can find that all the band-gaps for three different ribbon widths ($W = 8$, 9 and 10) display a zigzag oscillation as the strain t varies, and the change between two neighbouring turning points is nearly linear. However, the three curves exhibit distinct features with the variation of strain. As strength of tensile strain is enhanced, the band-gaps of A-BNNRs with $W = 8$ and 9 first increase and then decrease. While the gap of A-BNNR with $W = 10$ displays an opposite trend instead. Meanwhile, the maximal values of three curves are sensitive to the width of A-BNNR. Similar to the case of GNRs,[29] A-BNNRs also show a family behaviour with respect to the width ($W = 3n$, $3n + 1$, $3n + 2$).[14] As a comparison, the variations of various gaps of A-BNNRs with $W = 11$, 12, 13 with t are depicted in Fig. 5(b). Comparing Fig. 5(a) with Fig. 5(b), it is found that the band-gaps of A-BNNRs in a similar family such as $W = 8$ and 11 A-BNNRs, remain a similar trend with the variation of strain except for the maximal value and period shrinking. These results verify that the dependence of band-gap of A-BNNR on strain is determined by the ribbon width.

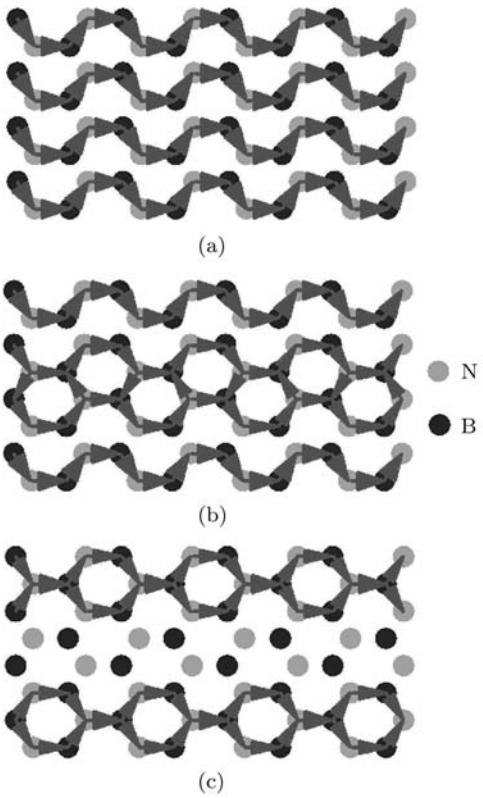


Fig. 4. Local current-density distribution (arrows) of A-BNNR with $W = 8$ under various values of strain t at $E = 3.45$ eV : $t = 0$ (a), 0.635 (b) and 0.8 eV (c), with grey and black balls denoting N and B atoms, respectively.

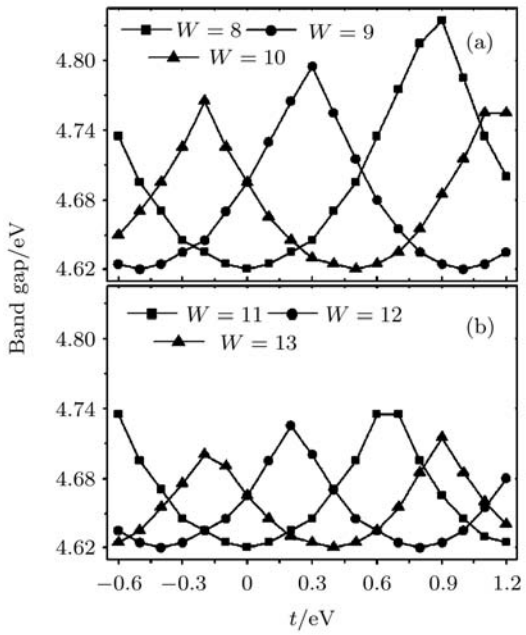


Fig. 5. Variations of the band-gaps for A-BNNRs with strain t for different values of width W: $W = 8$, 9, 10 (a), and 11, 12, 13 (b).

In addition, the conductances of Z-BNNR under different strains are shown in Fig. 6. By comparing Fig. 6 with Fig. 2, one can find that the conductance modification of Z-BNNR under strain is similar to that of A-BNNR. For example, the widths of the highest conductance steps become wide as compressive strain is exerted on Z-BNNR [see Fig. 6(a)] and A-BNNR [see Figs. 2(b) and 2(c)]. While a tensile strain is exerted [see Figs. 6(c) and 2(e)], the widths both turn narrow instead. But the modification of conductance of Z-BNNR is much smaller than that of A-BNNR under the same strains. Under a tensile strain, i.e., $t = 0.8$ eV, the highest step disappears and a dip emerges in conductance of A-BNNR. However, the highest step still exists in conductance of Z-BNNR even if a larger tensile strain (1.0 eV) is exerted. Therefore, the electron transport of the Z-BNNR under strain is not discussed in detail.

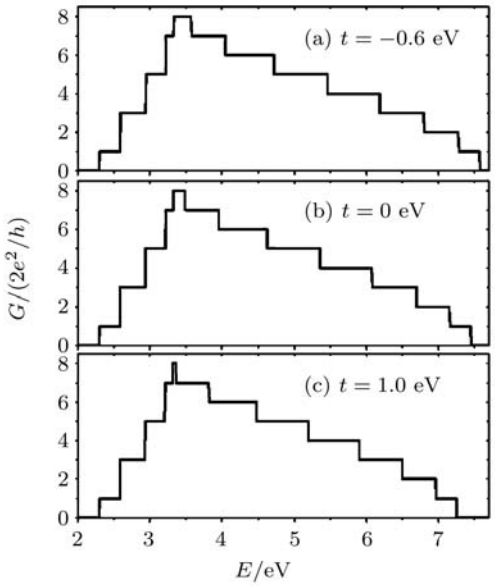


Fig. 6. Curves for conductance versus electron energy for Z-BNNR with $W = 8$ for three different values of strain t.

4. Conclusions

The transport properties of BNNRs under a uniaxial strain are investigated by the Green's function method. It is found that the position and the width of the conductance steps of A-BNNR are different under various strains. As the tensile strain is exerted, the highest conductance step becomes narrow and even disappears. Subsequently, a dip emerges. To explain these phenomena, the energy band structure and the local current density of the A-BNNR under strain are studied. The results show that all the sub-bands move upwards or downwards and the transmission channels change with tensile strain. Meanwhile, the band-gap of A-BNNR shows a zigzag oscillation under strain. In addition, the modification in conductance of Z-BNNR is similar to that of A-BNNR. But the effect of strain on the conductance of Z-BNNR is weaker than that of A-BNNR. These results are important for understanding and controlling the transport properties of BNNRs.

References

[1] Novoselov K S, Jiang D, Schedin F, Booth T J, Khotkevich V V, Morozov S V and Geim A K 2005 *Proc. Nat. Acad. Sci.* **102** 10451
[2] Han W Q, Wu L J, Zhu Y M, Watanabe K and Taniguchi T 2008 *Appl. Phys. Lett.* **93** 223103
[3] Pacilé D, Meyer J C, Girit Ç Ö and Zettl A 2008 *Appl. Phys. Lett.* **92** 133107
[4] Arnaud B, Lebegue S, Rabiller P and Alouani M 2006 *Phys. Rev. Lett.* **96** 26402
[5] Blase X, Rubio A, Louie S G and Cohen M L 1995 *Phys. Rev.* B **51** 6868
[6] Deng J X, Zhang X K, Yao Q, Wang X Y, Chen G H and He D Y 2009 *Chin. Phys.* B **18** 4013
[7] Han M Y, Özyilmaz B, Zhang Y B and Kim P 2007 *Phys. Rev. Lett.* **98** 206805
[8] Chen Z, Lin Y M, Rooks M J and Avouris P 2007 *Physica* E **40** 228
[9] Li X L, Wang X R, Zhang L, Lee S W and Dai H J 2008 *Science* **319** 1229
[10] Schniepp H C, Li J L, McAllister M J, Sai H, Herrera-Alonso M, Adamson D, Prud'homme R K, Car R, Saville D A and Aksay I A 2006 *J. Phys. Chem.* B **110** 8535
[11] Rollings E, Gweon G H, Zhou S Y, Mun B S, McChesney J L, Hussain B S, Fedorov A V, First P N, de Heer W A and Lanzara A 2006 *J. Phys. Chem. Solids* **67** 2172
[12] Yang X Y, Dou X, Rouhanipour A, Zhi L J, Rader H J and Mullen K 2008 *J. Am. Chem. Soc.* **130** 4216
[13] Novoselov K S, Geim A K, Morozov S V, Jiang D, Katsnelson M I, Grigorieva I V, Dubonos S V and Firsov A A 2005 *Nature* **438** 201
[14] Park C H and Louie S G 2008 *Nano Lett.* **8** 2200
[15] Pauli T K, Bhattacharya P and Bose D N 1990 *Appl. Phys. Lett.* **56** 2648
[16] Gui G, Li J and Zhong J X 2008 *Phys. Rev.* B **78** 75435
[17] Sun L, Li Q X, Ren H, Su H B, Shi Q W and Yang J L 2008 *J. Chem. Phys.* **129** 074704
[18] Li J, Gui G and Zhong J X 2008 *J. Appl. Phys.* **104** 094311
[19] Chen Y P, Xie Y E and Yan X H 2008 *J. Appl. Phys.* **103** 063711

[20] Jódar E, Pérez-Garrido A and Díaz-Sánchez A 2006 *Phys. Rev.* B **73** 205403
[21] Chen Y P, Yan X H, Lu M W and Deng Y X 2004 *Chin. Phys.* **13** 1537
[22] Guo W, Hu Y B, Zhang Y Y, Du S X and Gao H J 2009 *Chin. Phys.* B **18** 2502
[23] Nakamura J, Nitta T and Natori A 2005 *Phys. Rev.* B **72** 205429
[24] Sols F, Macucci M, Ravaioli U and Hess K 1989 *J. Appl. Phys.* **66** 3892
[25] Yan J Y, Zhang P, Sun B, Lu H Z, Wang Z G, Duan S Q and Zhao X G 2009 *Phys. Rev.* B **79** 115403
[26] Xu H Y, Heinzel T, Evaldsson M and Zozoulenko I V 2008 *Phys. Rev.* B **77** 245401
[27] Li J, Sun L Z and Zhong J X (Strain effects on the electronic and structural properties of boron nitride nanoribbons) (unpublished)
[28] Shi J R and Gu B Y 1997 *Phys. Rev.* B **55** 9941
[29] Brey L and Fertig H A 2006 *Phys. Rev.* B **73** 235411